*Journal of Thermal Analysis and Calorimetry, Vol. 68 (2002) 361–372*

# PHYSICO-CHEMICAL CHARACTERIZATION OF HYDRATED AND ANHYDROUS CRYSTAL FORMS OF AMLODIPINE BESYLATE

*J. M. Rollinger*[*] *and* *A. Burger*

Institute of Pharmacy/Pharmacognosy, University of Innsbruck, Innrain 52, Josef-Moeller-Haus, A-6020 Innsbruck, Austria

## Abstract

The antihypertensive drug substance amlodipine besylate crystallizes in two stable crystal forms, an anhydrate and a hitherto unknown monohydrate. Both forms have been characterized by thermal analysis, X-ray powder diffractometry, FTIR- and FT Raman spectroscopy. Moisture sorption- and desorption investigations reveal their unusual physical stability in a broad range of relative humidities. The monohydrate forms an isomorphic dehydrate upon dehydration, which was elucidated by variable temperature X-ray powder diffractometry. Physico-chemical properties as well as relative stabilities of the crystal forms are described and discussed based on a comprehensive analytical identification, and enable an estimation of practical relevance for manufacturing of amlodipine besylate solid dosage forms.

**Keywords:** amlodipine besylate, FTIR- and FT Raman spectroscopy, isomorphic dehydrate, monohydrate, pseudopolymorphism, thermal analysis, variable temperature X-ray powder diffractometry, water sorption

## Introduction

Amlodipine besylate (rINNM), (±)-3-ethyl-5-methyl-2-(2-aminoethoxymethyl)-4-(2-chlorophenyl)-1,4-dihydro-6-methyl-3,5-pyridinedicarboxylate benzenesulphonate (Fig. 1), belongs to the group of dihydropyridine calcium-channel blockers. It is used as the racemate in the management of angina pectoris and hypertension, for example in Norvasc®, Istin® or Amlor® [1], and is one of the world's most widely prescribed cardiovascular drugs [2]. As reported earlier, the tendency of dihydropyridines to crystallize in more than one crystal form is extensively high [3–7]. Both, polymorphism and pseudopolymorphism (solvated or hydrated forms) result in different physical properties of the respective crystal forms. Hence, they affect analytics as well as crucial pharmaceutical properties, such as density, morphology [8], relative

* Author for correspondence: Phone +43-512-507-5308; Fax: +43-512-507-2939; E-mail: judith.rollinger@uibk.ac.at

*1418–2874/2002/ $ 5.00*

*Akadémiai Kiadó, Budapest*
*Kluwer Academic Publishers, Dordrecht*

stability, dissolution rate, solubility [9], and finally the performance of a solid dosage form [10].

The present study deals with the physico-chemical characterization of (±)-amlodipine besylate crystal forms, an anhydrous form (AnH), a monohydrate (MH) and its dehydrated isomorphic form (DeH). Beside their thermoanalytical characterization, a specific aim was to investigate their physical stability and structural features with water vapor sorption- and desorption studies, X-ray powder diffractometry at variable temperatures, as well as FTIR- and FT Raman spectroscopy.

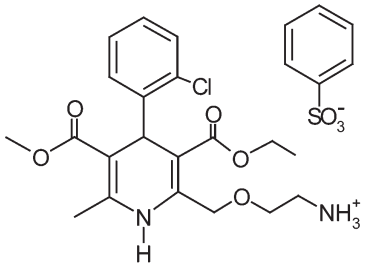


**Fig. 1** Molecular structure of amlodipin besylate

## Experimental

*Materials and solvents*

Available amlodipine besylate (Solvias AG, Basel, Switzerland) consisted of pure AnH. This anhydrous crystal form can also be obtained by crystallization experiments using organic solvents, whereas the MH crystallizes from aqueous solutions. Large quantities of the MH are easily obtained by stirring an aqueous suspension of the AnH (magnetic stirrer, 900 rpm, 24 h at ambient conditions). All solvents and chemicals used for this study were of analytical grade.

*Thermal analysis*

Hot stage microscopy was performed with a Reichert-Thermovar polarizing microscope and a Kofler hot-stage (Reichert, Vienna, Austria).

Differential scanning calorimetry (DSC) was carried out with a DSC-7 (Perkin Elmer, Norwalk, CT) using Pyris Software Ver. 2.0 for Windows. Sample masses for quantitative analysis were 1 to 3±0.0005 mg (Ultramicroscales UM3, Mettler, CH-Greifensee, Switzerland) weighed into perforated aluminum sample pans (25 μL). Nitrogen 5.0 (20 mL $min^{-1}$) was used as purge gas. The temperature axis was calibrated with benzophenone (*m.p.* 48.0°C) and caffeine (*m.p.* 236.2°C). Enthalpy calibration of the DSC signal was performed with indium 99.999% (Perkin Elmer, Norwalk, CT). The applied heating rate (HR) was 5 K $min^{-1}$.

Thermogravimetry (TG) was carried out with a TGA-7 instrument (Perkin Elmer, Norwalk, CT) using 50 μL platinum sample pans and a nitrogen purge (nitro-

gen 5.0, balance purge: 40 mL $min^{-1}$, sample purge: 20 mL $min^{-1}$). The sample mass was in the range of 1 to 5±0.0005 mg and the heating rate was 5 K $min^{-1}$. Mass calibration was performed with 100 mg calibration mass (Perkin Elmer), temperature calibration with alumel (magnetic transition temperature 163.0°C) and nickel (magnetic transition temperature 354.0°C).

*X-ray powder diffraction (XRPD)*

XRPD patterns were obtained with a Siemens D-5000 X-ray diffractometer (Siemens AG, Karlsruhe, Germany) equipped with θ/θ-goniometer, a Göbel mirror (Bruker AXS, Karlsruhe, Germany), a 0.15° soller slit collimator, and a scintillation counter. The patterns were recorded at a tube voltage of 40 kV, and a tube current of 35 mA, applying a scan rate of 0.005° 2θ $s^{-1}$ in the angular range of 2 to 40° 2θ. For variable temperature X-ray powder diffraction the samples were stored in a low temperature camera (TTK Anton Paar KG, Kat.Nr.57478, Graz, Austria). A heating rate of 10 K $min^{-1}$ was used to the desired temperature, which was maintained for the analysis period (from 2 to 40°, 0.020° 2θ $s^{-1}$, 31.7 min). The patterns were collected at 0% relative humidity (RH) using an air purge, dried over silicagel and phosphorus pentoxide before the sample chamber.

*FTIR spectra*

FTIR spectra were recorded with a Bruker IFS 25 FTIR-spectrometer (Bruker Analytische Messtechnik GmbH, Karlsruhe, Germany) connected with a Bruker FTIR-microscope (15x Cassegrain-objective and visible polarization). Samples were scanned as potassium bromide pellets (diameter 13 mm; 1 mg amlodipine besylate to 270 mg potassium bromide; pressure 740 MPa) at an instrument resolution of 2 $cm^{-1}$ in the spectral range from 4000 to 600 $cm^{-1}$ (50 interferograms per spectrum). For FTIR-microscopy, small samples were rolled on a zinc selenide window (13×2 mm) and recorded at an instrument resolution of 4 $cm^{-1}$ (focus diameter 50 μm, 100 interferograms per spectrum).

*FT-Raman spectra*

FT-Raman spectra were recorded with a Bruker RFS 100 FT-Raman spectrometer (Bruker Analytische Meßtechnik GmbH, Karlsruhe, Germany) equipped with a diode-pumped Nd:YAG laser (1064 nm) as the excitation source and a liquid nitrogen-cooled high-sensitivity detector. The powder samples were packed into small aluminum cups, and the spectra were recorded at an output power of 200 mW (64 scans at 4 $cm^{-1}$ instrument resolution).

*Sorption kinetics*

The determination of moisture uptake was studied gravimetrically at 25°C and 92% RH, using special hygrostates [11] and a below-weighing balance (Mettler semi-mi-

cro balance AT 261, Mettler Instruments AG, CH-Greifensee). The sample mass was about 250 to 300 mg. RH in the semi-micro hygrostates was adjusted with dried silica gel or phosphorus pentoxide ($P_2O_5$, RH 0%), and saturated salt solution of potassium nitrate (RH 92%) at 25°C.

## Results

*Physico-chemical characterization of the crystal forms*

The most important physico-chemical parameters of the amlodipine besylate crystal forms are summarized in Table 1.

**Table 1** Physico-chemical data of amlodipine besylate crystal forms

| Crystal form | | AnH | DeH | MH |
|---|---|---|---|---|
| Preparation by | | Crystallization from organic solvents | Dehydration of MH at 0% RH, 50 to 70°C | Crystallization from aqueous solution or suspension (AnH) |
| *M.p.*: | TM/°C | 197.5–200 | 85.0–100 | 70–100 |
| | DSC onset/°C | 198 | 88 | 70–100 |
| | DSC peak/°C | 200 | 93 | 80–110 |
| Enthalpy of fusion/kJ $mol^{-1}$ [a] | | 44.1±3.6 | 9.7 [b] | 60.1±5.4 [c] |
| Entropy of fusion/J $mol^{-1}$ $K^{-1}$ [a] | | 93.7±7.6 | 26.9 [b] | – |
| Content of water/% | | <0.1 | <0.1 | 2.9– 3.1 |
| Characteristic FTIR frequencies/$cm^{-1}$ | | – | – | 3550–3350 |
| | | 3301 | 3305 | 3311 |
| | | 3156 | 3063 | 3061 |
| | | 1698 | 1690 | 1689 |
| | | 1676 | – | – |
| | | – | 1650 | 1648 |
| | | 1616 | 1608 | 1607 |
| | | 1494 | 1484 | 1485 |
| | | 1445 | 1445 | 1446 |
| | | 1433 | 1436 | 1436 |
| | | 1366 | 1347 | 1348 |
| | | 1303 | 1306 | 1308 |
| | | – | 1287 | 1288 |
| | | 1265 | 1260 | 1261 |

[a]±95% C.I.; [b]single value; [c]enthalpy of fusion inclusive enthalpy of dehydration

## Thermal analysis

AnH consists of colorless, small needles and prisms of about 50 to 100 μm length, showing a melting interval between 197.5 and 200°C (Fig. 2a). Decomposition is visible at temperatures >190°C indicated by a brown coloration. The melt is thermally unstable. Thermogravimetrically, a distinct and continuous mass loss is observed beyond the melting range. Due to the decomposition, the crystallization of polymorphic forms from the supercooled melt was not feasible.

The micro crystalline aggregates of the MH dehydrate and melt simultaneously between 70 and 100°C. The TG-curve shows a reproducible mass loss of 2.9 to 3.1% in this temperature interval (Fig. 2d), which corresponds to one molecule of water per molecule amlodipine besylate (theoretical value: 3.08%). Figure 2b shows the DSC-trace of a MH sample, containing crystal seeds of the AnH. The endothermic dehydration and melting process of the MH is directly followed by the exothermic crystallization process of the AnH (inhomogeneous melting). However, the combined process (dehydration and melting) proceeds homogeneously, if no crystal seeds of the AnH are present in the MH sample. Figure 2c shows the corresponding DSC-run of the MH. P1 represents the dehydration and fusion reaction. Between P1 and P2 the substance is amorphous (liquid), which was confirmed by hot stage microscopy, FTIR-microscopy, and XRPD. At about 140°C an exothermic crystallization of the AnH (P2) and finally its melting at about 190°C (P3) take place. The enthalpy of fusion and melting range of this AnH are significantly decreased (compare Fig. 2a and b). This behavior can be explained by a thermal instability of the amorphous state, which existed from about 90 to 140°C (Fig. 2c, P1 to P2).

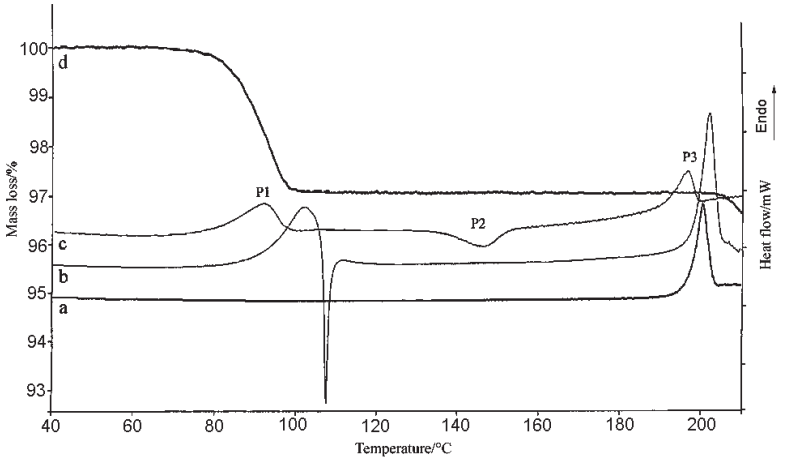


**Fig. 2** DSC-curve of the AnH (a); DSC-curve of the MH with inhomogeneous melting (b); DSC-curve of the MH with homogeneous melting (c); TG-curve of the MH (d)

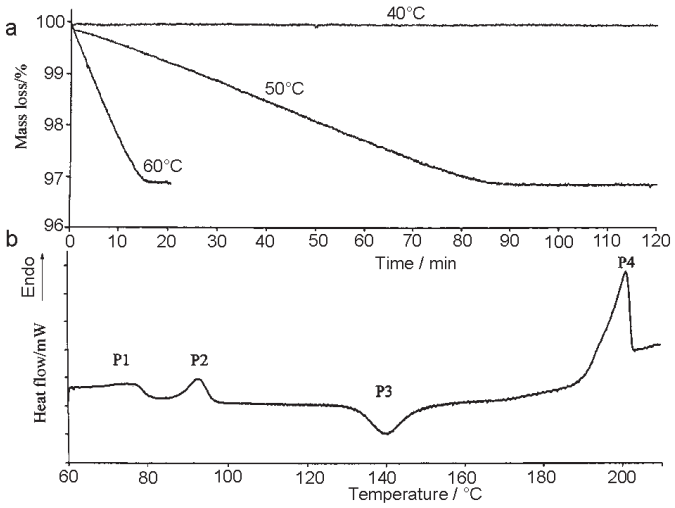


**Fig. 3** Isothermal TG-curves of the MH at 40, 50, and 60°C, respectively (a); DSC-curve of in situ prepared DeH (1 h, 60°C) starting with the MH (b)

In addition, isothermal TG investigations were carried out to gain an insight in the thermal stability of MH. At temperatures of 25, 30 , and 40°C (0% RH) no significant loss of water was observed within 6 h (mass loss <0.2%). However, at 50°C and 60°C the crystal water continuously escapes within 90 min and 17 min, respectively (Fig. 3a). The obtained products quickly reuptake moisture after opening the TG-oven. The process of re- and dehydration is reversible at temperatures below the melting range of this crystal form (<75°C). Thus, the two processes of dehydration and melting could be separated. In analogy to the TG-measurements, MH was kept isothermally at 60°C (under nitrogen purge) for one hour in an open DSC Alu-pan to release its crystal water without destroying the crystal structure. When heated with a rate of 5 K $min^{-1}$, last traces of water are removed below 75°C (P1). The melting of the dehydrated material (DeH) starts at 88°C (P2), followed by the crystallization of AnH at about 130°C (P3) and its decreased melting at about 190°C (P4). The enthalpy of fusion of DeH is 9.7 kJ $mol^{-1}$, which represents an extremely low value for an enthalpy of fusion probably due to an extensive loss in lattice energy while the water is released from the crystal lattice.

## Sorption and desorption measurements

AnH was stored over 92% RH at 25°C for almost 2 months without a significant water uptake (<0.1%, Fig. 4a). On the other hand, MH showed no release of water by storage over dried silica gel (0% RH, Fig. 4b), which is in accordance with isothermal TG investigations at 25°C. Surprisingly, the dehydration occurs within 6 days under the same conditions, when phosphorus pentoxide is used as a drying agent (Fig. 4c). The rehydration of the previously formed DeH takes only a few minutes, when stored

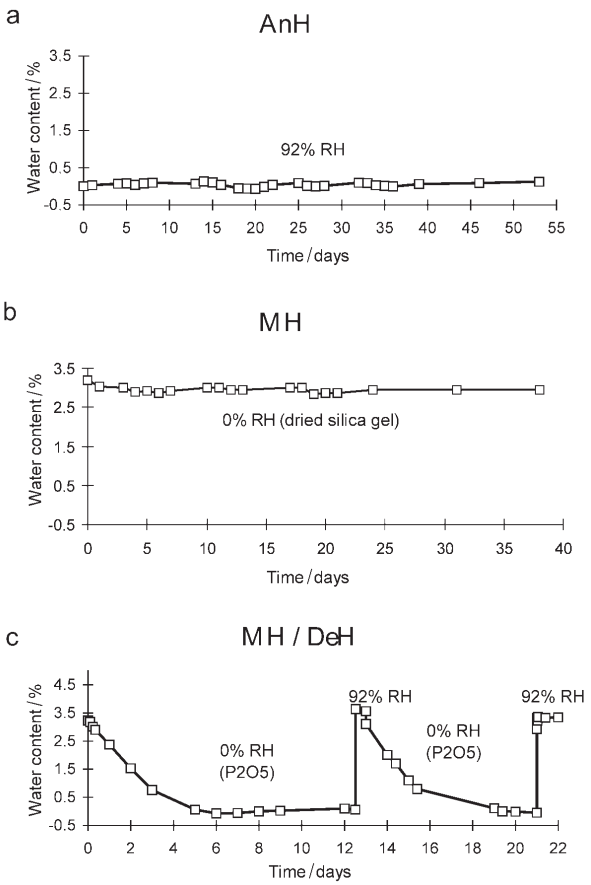


**Fig. 4** Water sorption and desorption of amlodipine besylate crystal forms at 25°C

over 92% RH. This re- and dehydration process is reproducible as demonstrated in Fig. 4c. The crystal lattice is essentially maintained during loss or uptake of water, which was proved by FTIR-microscopy and X-ray powder diffractometry.

## Vibrational spectroscopy

FTIR-spectra of AnH and MH were recorded with the potassium bromide method, whereas the spectrum of DeH could only be obtained by FTIR-microscopy. In order to dehydrate MH, the sample was purged for 1 h with nitrogen 5.0 at 65°C before and during recording FTIR-micro-spectrum. As shown in Fig. 5, the spectra of MH and DeH are essentially the same, except for the water absorption bands in the O–H-stretching region between 3550 and 3350 $cm^{-1}$ in the spectrum of MH.

In Table 1 the most characteristic FTIR frequencies are listed. Small differences within the three forms are observed for the $–NH_2$ stretching vibration at about

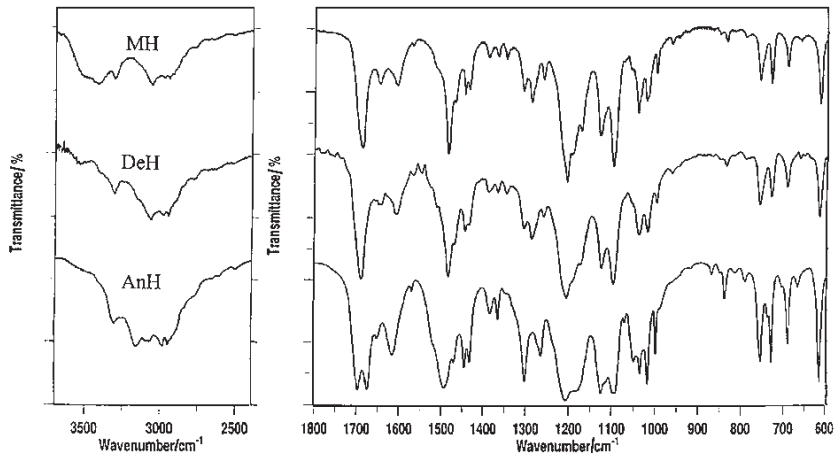


**Fig. 5** FTIR-spectra of amlodipine besylate crystal forms. AnH (potassium bromide method) (a); DeH (in situ prepared from MH, 1 h, 65°C, 0% RH) on zink selenide window (b); MH (potassium bromide method) (c)

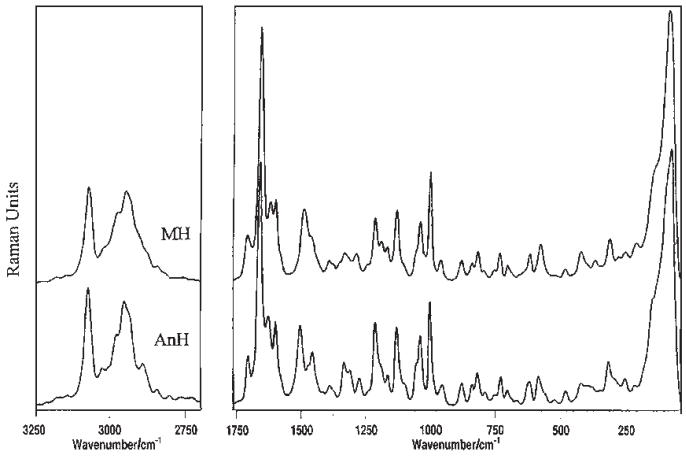


**Fig. 6** FT Raman-spectra of amlodipine besylate AnH and MH

3300 $cm^{-1}$. However extensive differences exist between the spectra of the AnH and the other forms (MH and DeH), especially in the range of C–H– and $NH_3^+$-stretching vibrations between 2900 and 3200 $cm^{-1}$, in the C=O stretch of the carbonyl groups (1676 to 1700 $cm^{-1}$), as well as in the fingerprint region.

FT Raman spectra of AnH and MH were recorded at ambient conditions (Fig. 6). Reproducible differences can be observed in the aromatic and aliphatic C–H stretching bands between 3250 and 2750 $cm^{-1}$ (AnH: 3067, 2948 $cm^{-1}$; MH: 3065, 2943 $cm^{-1}$), and in the range of C=O and C=C stretching vibrations (AnH: 1651, 1617 $cm^{-1}$; MH: 1647, 1610 $cm^{-1}$). Distinct shifts and intensity differences are found in the region of aliphatic and N–H bending vibrations (AnH: 1495, 1449 $cm^{-1}$; MH:

1481, $1451_{weak}$ $cm^{-1}$) indicating an involvement of the dihydropyridine side chains in position 2 and 3 in the different molecular arrangements of AnH and MH. Although the differences of the Raman spectra are less striking than FTIR results, highly reproducible spectra are obtained for these two crystal forms.

## X-ray powder diffractometry

X-ray powder diffractograms of AnH and MH (Fig. 7) show distinct differences in the positions and relative intensities of the reflections (Table 2), clearly indicating different crystal lattices. Unfortunately, no crystal structures of amlodipine besylate have been solved up to now because of their small size. In order to record any changes in the crystal

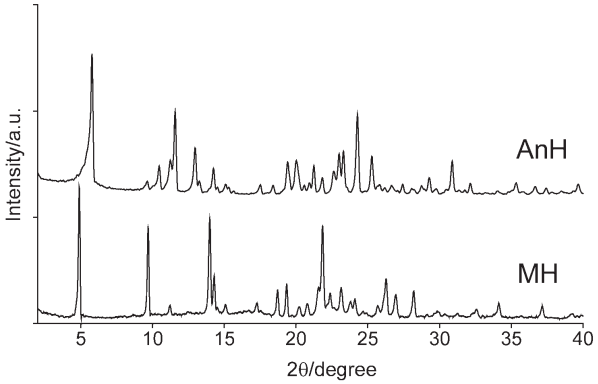


**Fig. 7** X-ray powder patterns of amlodipine besylate AnH and MH

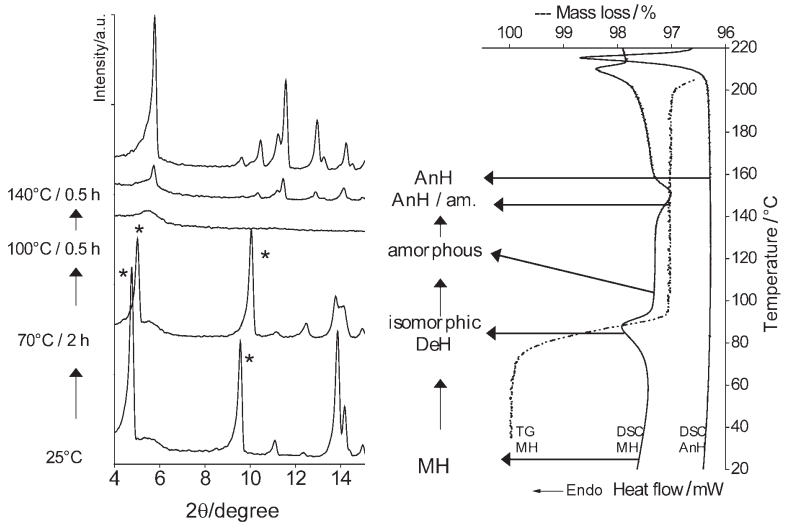


**Fig. 8** Left side: variable temperature X-ray powder diffraction at 0% RH, starting with the MH (bottom); Right side: TG- and DSC-curves of corresponding crystal forms

lattice of the MH upon heating, its XRPD pattern between 4 and 15° 2θ was recorded at different temperatures and 0% RH (Fig. 8, left side from bottom up). For correlation, the different patterns are shown together with the corresponding TG- and DSC-curves (Fig. 8, right side). On heating up MH (70°C, 2 h), the crystals release their water essentially retaining the three-dimensional order of the parent hydrate, which is apparent through similarities in XRPD patterns. However, there are some considerable shifts of the peak positions of MH toward higher 2θ (labeled with asterisks in Fig. 8, +0.26° and +0.48° 2θ differences, respectively) in the diffraction pattern of DeH, caused by a distinct contraction of the corresponding unit cell dimensions. On the other hand, the 2θ positions between 10 and 15° 2θ are more or less unaffected by the dehydration process and vary only between –0.1° and +0.1° 2θ. This clearly indicates an anisotropic shrinkage of the lattice upon dehydration. Further heating up to 100°C leads to the melting of the isomorphic DeH followed by a crystallization process of the melt at about 140°C. The resulting pattern is characterized by definite peak positions of AnH. For comparison, the powder pattern of AnH is depicted on the top of Fig. 8. The obtained results show that the transformation from DeH to AnH does not occur in the solid state, but via the melt.

**Table 2** Two theta positions (2θ), *d*-spacings (*d*) and relative intensities (*I*) of X-ray powder diffraction patterns of AnH and MH

| AnH | | | MH | | |
|---|---|---|---|---|---|
| 2θ/° | *d*/Å | *I*/% | 2θ/° | *d*/Å | *I*/% |
| 5.907 | 14.9499 | 100.0 | 4.889 | 18.0616 | 100.00 |
| 10.583 | 8.3525 | 9.08 | 9.691 | 9.1195 | 69.83 |
| 11.358 | 7.7838 | 9.31 | 11.209 | 7.8871 | 13.22 |
| 11.705 | 7.5542 | 33.45 | 13.985 | 6.3274 | 76.12 |
| 13.105 | 6.7503 | 14.52 | 14.283 | 6.1958 | 32.36 |
| 13.369 | 6.6174 | 4.87 | 17.262 | 5.1328 | 13.67 |
| 14.368 | 6.1593 | 7.67 | 18.712 | 4.7382 | 22.70 |
| 15.223 | 5.8156 | 3.75 | 19.346 | 4.5843 | 28.08 |
| 19.520 | 4.5438 | 4.64 | 20.789 | 4.2693 | 13.76 |
| 19.654 | 4.5131 | 5.79 | 21.570 | 4.1164 | 25.07 |
| 20.145 | 4.4042 | 7.79 | 21.848 | 4.0647 | 68.64 |
| 21.378 | 4.1529 | 5.83 | 22.371 | 3.9709 | 21.60 |
| 21.967 | 4.0429 | 4.29 | 23.146 | 3.8396 | 24.43 |
| 22.753 | 3.9049 | 6.41 | 23.786 | 3.7376 | 14.04 |
| 23.128 | 3.7912 | 11.43 | 24.099 | 3.6899 | 16.50 |
| 23.445 | 3.7912 | 11.43 | 26.271 | 3.3895 | 31.27 |
| 24.399 | 3.6452 | 16.70 | 26.944 | 3.3064 | 19.42 |
| 25.414 | 3.5018 | 9.52 | 28.193 | 3.1627 | 23.61 |
| 31.006 | 2.8819 | 6.79 | 34.133 | 2.6246 | 14.49 |

## Discussion

XRPD experiments indicate that there is hardly any reorganization of the crystal lattice during dehydration of MH apart from an anisotropic crystal shrinkage. This suggests (a) a not very rigid crystal lattice, and (b) the existence of voids in the form of channels or planes in MH, which are exclusively occupied by water molecules. Such phenomena are often observed in hydrates and solvates, subsumed under the term isomorphic desolvate or dehydrate [10, 12]. However, a destructive process upon water loss of amlodipine besylate takes place while heating up MH at ambient conditions. The dehydration and the collapse of the three dimensional order occur simultaneously. On the other hand, the exposition of MH over phosphorus pentoxide at 25°C or to elevated temperatures (65 to 70°C) at 0% RH (nitrogen 5.0 purge or dried silica gel) results in a cooperative departure of water [13, 14] and formation of an isomorphic dehydrate (DeH). The loss of water and the creation of void spaces in crystal lattice finally lead to a reduced packing efficiency and a less stable crystal lattice [15], as demonstrated by the low enthalpy of fusion of DeH (9.7 kJ $mol^{-1}$). In order to increase the packing density and to gain a higher stability, two possible lattice compensations are commonly observed [12]: the relaxation in the sense of a crystal shrinkage and/or the incorporation of solvent, which mainly corresponds to an extensively high hygroscopicity of the desolvated material. In the case of amlodipine besylate, both stabilization processes are clearly visible by variable temperature XRPD- and water sorption-desorption investigations. The results indicate that the water molecules are tightly held in MH over the whole range of RH at 25°C, not showing any tendency for an additional uptake at higher RH values or loss of 3% water at 0% RH. Therefore, MH is characterized by a stoichiometric relationship of 1:1, amlodipine besylate to water. At room temperature extremely dry conditions are required for the dehydration of MH, which can only be achieved with phosphorus pentoxide, but not with silica gel. At ambient conditions DeH stabilizes its crystal structure within a few minutes by reabsorbtion of water from the atmosphere (Fig. 4c).

## Conclusions

Amlodipine besylate crystallizes from organic solvents as AnH, which represents the thermodynamically stable crystal form of this compound. However, from aqueous solutions or suspensions a stable monohydrate (MH) is obtained. Under extreme conditions (0% RH, 50 to 70°C), this pseudopolymorphous crystal form is enabled to completely release its water in retaining its crystal lattice and forming an isomorphous dehydrate (DeH). It has been shown that thermal analysis in combination with variable temperature XRPD and moisture sorption-desorption measurements are valuable tools for the investigation of the dehydration behavior.

Both, AnH and MH, show a high stability at ambient conditions and are easily identified by vibrational spectroscopy and XRPD. These features are requirements for a well-directed application of a respective crystal form in solid dosage forms. Because of the stability at high moisture conditions and a thermal stability up to 190°C,

AnH should be the crystal form of choice for manufacturing. In addition, anhydrates generally show a higher aqueous solubility and dissolution rate than the respective hydrates. Since amlodipine besylate is a slightly soluble drug substance, the usage of AnH is also advisable from biopharmaceutical point of view.

* * *

The authors thank Solvias AG, Basel, Switzerland, for supplying (±)-amlodipine besylate. Helpful discussions with Dr. Ulrich Griesser are gratefully acknowledged.

## References

1 Martindale, The Extra Pharmacopoeia, Royal Pharmaceutical Society, 1999.
2 RxList: The Top 200 Prescriptions for 2000 by Number of US Prescriptions Dispensed, http://www.rxlist.com (2001).
3 A. Grunenberg, B. Keil and J.-O. Henck, Int. J. Pharm., 118 (1995) 11.
4 A. Burger and K. T. Koller, Sci. Pharm., 64 (1996) 293.
5 A. Burger, J. M. Rollinger and P. Brüggeller, J. Pharm. Sci., 86 (1997) 674.
6 F. Hirayama, M. Honjo, H. Honjo, H. Arima, K. Okimoto and K. Uekama, Eur. J. Pharm. Sci., 11 (2000) 81.
7 J. M. Rollinger and A. Burger, J. Pharm. Sci., 90 (2001) 949.
8 K. R. Morris, S. L. Nail, G. E. Peck, S. R. Byrn, U. J. Griesser, J. G. Stowell, S.-J. Hwang and K. Park, PSTT, 1 (1998) 235.
9 A. Burger and R. Ramberger, Mikrochim. Acta, 1979 II (1979) 259.
10 S. Byrn, R. Pfeiffer, M. Ganey, C. Hoiberg and G. Poochikian, Pharm. Res., 12 (1995) 945.
11 U. J. Griesser and A. Burger, Int. J. Pharm., 120 (1995) 83.
12 G. A. Stephenson, E. D. Groleau, R. L. Kleemann, W. Xu and D. R. Rigsbee, J. Pharm. Sci., 87 (1998) 536.
13 S. Petit and G. Coquerel, Chem. Mat., 8 (1996) 2247.
14 C. Habare, S. Petit and G. Coquerel, PhandTA 4, Karlsruhe Workbook KC 5 (1999).
15 A. I. Kitaigorodsky, Molecular Crystals and Molecules, Academic Press, New York, London 1973, p. 184.
16 E. Shefter and T. Higuchi, J. Pharm. Sci., 52 (1963) 781.
17 A. Burger and U. J. Grießer, Eur. J. Pharm. Biopharm., 37 (1991) 118.